

Special Section on VCBM 2021

Longitudinal visualization for exploratory analysis of multiple sclerosis lesions

Sherin Sugathan^{a,*}, Hauke Bartsch^{a,d}, Frank Riemer^b, Renate Grüner^d, Kai Lawonn^c,
Noeska Smit^{a,b,d}

^a Department of Informatics, University of Bergen, Norway

^b Mohn Medical Imaging and Visualization Centre, Norway

^c Institute for Computer Science, University of Jena, Germany

^d Haukeland University Hospital, Norway

ARTICLE INFO

Article history:

Received 2 April 2022

Received in revised form 25 July 2022

Accepted 25 July 2022

Available online 29 July 2022

Keywords:

Multiple sclerosis

Longitudinal visualization

Lesion analysis

Magnetic resonance imaging

White matter lesions

ABSTRACT

In multiple sclerosis (MS), the amount of brain damage, anatomical location, shape, and changes are important aspects that help medical researchers and clinicians to understand the temporal patterns of the disease. Interactive visualization for longitudinal MS data can support studies aimed at exploratory analysis of lesion and healthy tissue topology. Existing visualizations in this context comprise bar charts and summary measures, such as absolute numbers and volumes to summarize lesion trajectories over time, as well as summary measures such as volume changes. These techniques can work well for datasets having dual time point comparisons. For frequent follow-up scans, understanding patterns from multimodal data is difficult without suitable visualization approaches. As a solution, we propose a visualization application, wherein we present lesion exploration tools through interactive visualizations that are suitable for large time-series data. In addition to various volumetric and temporal exploration facilities, we include an interactive stacked area graph with other integrated features that enable comparison of lesion features, such as intensity or volume change. We derive the input data for the longitudinal visualizations from automated lesion tracking. For cases with a larger number of follow-ups, our visualization design can provide useful summary information while allowing medical researchers and clinicians to study features at lower granularities. We demonstrate the utility of our visualization on simulated datasets through an evaluation with domain experts.

© 2022 The Authors. Published by Elsevier Ltd. This is an open access article under the CC BY license (<http://creativecommons.org/licenses/by/4.0/>).

1. Introduction

Multiple Sclerosis (MS) is a disease that affects the central nervous system. In MS, the immune system attacks the protective layer, called myelin, around the nerves, causing damage and disruption in nerve functionality [1]. The damaged areas are referred to as lesions and appear as scar-like features in medical images as shown in Fig. 1(a). Depending on the lesion type, location, and other characteristics, MS patients may experience a wide range of problems. Based on the symptoms developed by a patient, a clinician performs diagnosis and also makes a disability quantification using methods such as the Expanded Disability Status Scale (EDSS) [2]. For diagnosis, Magnetic Resonance Imaging (MRI) is a commonly used technique, where the clinicians can see the MS lesions as either bright or dark spots in the image depending on the MRI modality used. It is important to note that there is currently no permanent cure for

MS, but clinicians rely on medication-based disease management. Patients also undergo follow-up MRI scans, where clinicians assess medical images to see the clinical impact of medications. During follow-up, it is a common practice to compare the current scan with a previous scan. This involves matching both image slice locations and lesions between two time points to assess the difference. The process becomes difficult if there is a high lesion load and/or there are many follow-up scans. The complexity will further increase when users also need to track lesion information, e.g., new lesions, growth, and intensity changes, in multimodal or multiparametric datasets. Fig. 1(b) and (c) show an example lesion surface variation between a baseline and follow-up scan, respectively.

Fig. 2 shows an abstract depiction of the lesion change/event profiles such as shrinking, enlargement, merging, splitting and the appearance of new lesions.

Analysis of lesion load [3] across time points is important because it helps to assess the outcomes of MS disease management through the use of medications. Analyzing lesion information longitudinally across multiple datasets and modalities also needs

* Corresponding author.

E-mail address: sherin.sugathan@uib.no (S. Sugathan).

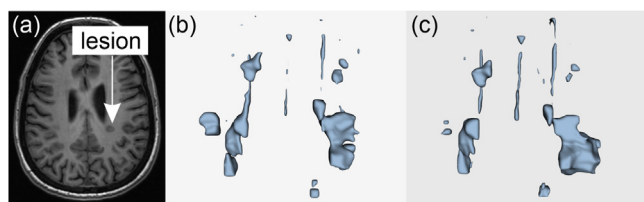


Fig. 1. (a) An axial view of a brain scan of a patient with multiple sclerosis reveals lesions as intensity differences, (b) lesion surfaces at a baseline scan, and (c) lesion surfaces at a follow-up scan.

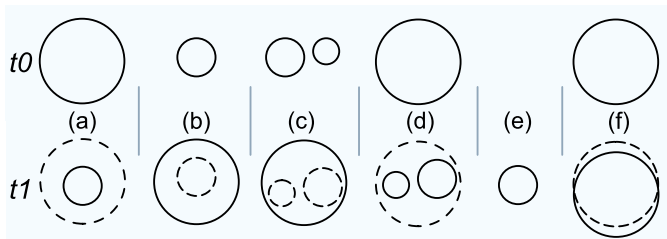


Fig. 2. An abstract representation of possible lesion changes and events possible between two scans taken at time t_0 and t_1 . (a) shrinking lesion, (b) enlarging lesion, (c) merging lesions, (d) splitting lesions, and (e) new lesion. The dotted curves in t_1 represent overlays, showing t_0 lesions.

to follow standards like the McDonald criteria [4]. For a diagnosis based on the McDonald criteria, it is important to understand the dissemination of lesions in space and time along with intensity variations. When using the diagnostic criteria, clinicians consider conventional slice views as an excellent mechanism for evaluating a patient. However, for conducting an explorative analysis on MS in a research context, advanced visualization tools can offer an advantage over conventional techniques. This is mainly due to the fuzzy nature of the disease. Similar to an iterative prototyping process, we received feedback during different stages of development from a collaborating neuroradiologist with clinical and research experience. The feedback collection during the development phase helped in guiding the visualization development. Other collaborators with the subject expertise were available throughout the development of the project. Realizing the possibilities of better tools for longitudinal MS analysis, we present an application that incorporates interactive visualizations to support lesion exploration and research.

In this design study, we consider the following as the main contributions:

- A stack plot-centered visualization design for exploratory analysis of lesion development over time.
- Auxiliary node graph representation of longitudinal MS data to handle complex analysis.
- An interactive visualization for individual spatial exploration of lesions.

2. Related work

There is a large body of related work focussing on visual analytics for temporal data, such as the work by Zhang et al. [5], which is a good example where they visualize time-varying data and showcase the benefits of linked plots. The work by [6] provides a good coverage of challenges involved in multimodal medical data visualization. Our focus is mainly on the visualization approaches for spatio-temporal MS data in particular.

2.1. Approaches for MS lesion data

Visualization approaches for MS longitudinal data so far focused on visualizing the lesion changes in ways that are suitable for further statistical analysis. On a high level, we put emphasis on presenting detailed lesion features from multi-modal datasets for easy exploration and discovery of patterns. The work by [7] is an example, where they fight the problem of high dimensionality and complexity of the data space. Adding to our motivation to do this study, Mainero et al. [8] states that any improvements made to visualization of MS lesions is extremely valuable for monitoring longitudinal lesion dynamics and for understanding their relations with their contribution towards neurodegeneration and to the establishment of irreversible disability.

The work by Okuda et al. [9] explores the need for studying lesion shape changes or shape evolution in the classification of chronic MS lesions. They visualize lesion differences only between two time points by providing both mesh- and glyph-based visualization. In contrast to their approach, we use a view-synchronized combination of mesh- and contour-based visualization. We did not use arrow glyphs in our visualization design, as glyph geometry adds to the visual scene complexity, especially for complex-shaped lesions. The work by [10] explores inter lesion relationships. In our work, we focus on tracking individual lesions. Fartaria et al. [11] perform statistical analysis of lesion changes. Their visualization mainly conveys lesion distribution information at a single time point. They employ similar visualizations as depicted in Fig. 3(b). The challenge with such a visual representation is that it is not a suitable visualization for representing data from multiple time points.

Kuckertz et al. [12] propose a system for automated monitoring of lesion evolution. In contrast to our method, they use a tree data structure with repeated nodes that represents the same lesion. Tory et al. [13] present multiple approaches to visualize longitudinal lesions. One of their approaches includes the use of 3D surface rendering, where they display each time step as an animation. As the complexity of reading the scene increases (as shown in Fig. 4) with an increasing number of time points and lesions, this approach is not suitable in our context. As visible in Fig. 4(c), the aggregation of data in the same scene is not a suitable visualization choice, especially when there are many follow-up scan data points with many lesions. In contrast to this approach, our visualization provides an interactive lesion-wise analysis of shape changes. The work by Köhler et al. [14] is a closely related visualization approach intended for longitudinal lesion data. After tracking the lesions over multiple follow-up scans, they visualize the lesions in a way that is analogous to what we depict in Fig. 3(a). Such bar charts works well if the number of follow-up scans available is low, however, it does not scale. For datasets including a larger number of follow-up scans like Filippi et al. [15], the cognitive load to understand the chart becomes high. Also, the visualization does not support studying the total lesion volume trend over time because every separate grouping in the bar chart represents a single lesion. People who are involved in MS lesion research can consider more follow-up cases than usual or even make research datasets through frequent follow-up scans. The work by Brune et al. [16] has developed into a commercial application supporting lesion analysis along with visualization of longitudinal data. Interestingly, they also make use of a bar chart-based visualization similar to what we depict in Fig. 3(c). In their work, they only compare the current and the previous scan. In contrast to the approaches in Köhler et al. [14], Fartaria et al. [11], and Brune et al. [16], our visualization application provides support for the explorative analysis of MS lesions which scales to datasets with a larger number of follow-ups.

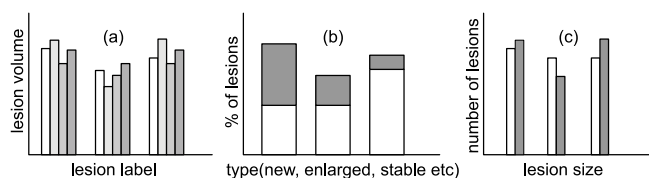


Fig. 3. Examples of current standards in longitudinal MS lesion visualization. (a) Each bar grouping represents the baseline and three follow-up scans for a specific lesion [14]. (b) Stacked bar chart representing lesions from cortical and white matter regions [11]. (c) The pair in every bar grouping indicates the current scan and prior scan size per lesion [16].

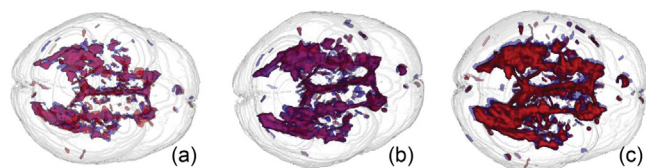


Fig. 4. Surface rendering of longitudinal lesions [13] where surfaces from multiple time points are rendered together in the same window (a) 2 time steps (b) 4 time steps and (c) all 11 time steps.

2.2. Approaches for spatio-temporal medical data

Several visualization studies have focused on improving the understanding of longitudinal medical datasets. For improved visual exploration capabilities, the work by Meuschke et al. [17] shows approaches for visualization of scalar fields using multiple linked abstract visualizations. Our work, in contrast, involves visualization of surface variations. Busking et al. [18] evaluate different methods for visually representing shape differences. While they focus on representing changes using contours generated from intersecting surfaces, we use a combination of surfaces on which we depict change in one of our visualizations. The reasons for avoiding point correspondence glyphs in our approach include an increased scene complexity and the incompatibility with handling the significant topology variations for lesions. Furmanova et al. [19] visualize the anatomical variability of structures using contours bands in order to represent a group of patients. In our application, we focus instead on visualizing time-varying data for a single subject, where we communicate lesion variability using contours and meshes along with a high-level brain structure context. Hermann et al. [20] present a detailed study on visualizing large deformations and variability in biomedical images. Instead of using glyphs, they have used a streamline visualization. In addition, they present change information using volume rendering and combination of contour and isosurface to visualize change. In our visualization tool, we use a combination of 2D contours and 3D meshes that are color-coded to show previous and current time points. Murugesan et al. [21] visualize time-varying brain data by clustering brain regions. They represent cluster evolution by using a node graph with an associated time axis. We associate a time axis only for our stack plot visualization. The work by Glaßer et al. [22] includes visualization of longitudinal tumor volume data using time intensity curves. For visual analysis, they use a mask-based segmentation of color-mapped 2D tumor slice data. Those maps are not suitable for a superimposed display. In contrast to their approach of visualizing the pathology and the context in the same scene, we separate them into separate scenes considering workflow-related benefits. Smith et al. [23] offer visualizations similar to stack plots, but they show information represented in a tree data structure. They have abstract visualizations that are manually linked to an anatomical image. In our visualizations, we primarily use the stack plot to convey

information on total lesion load, and we use automatic linking for connecting visualizations to a 3D anatomical context. To depict the evolutionary history of tumor samples, the work by Alves et al. [24] visualizes abstract changes that capture evolution and change information in a tree. We make use of a directed node graph for visualizing lesion evolution along with their properties encoded as node sizes and colors.

2.3. Approaches for other spatio-temporal data

There exists extensive literature on visualization approaches that are used in non-medical domains. In the work by Reh et al. [25], the tracking graph that is horizontally laid out includes repeated nodes to show tracking. Such an approach is not applicable in our context as we need to capture long follow-up information. The work by Diehl et al. [26] includes the use of multiple abstract visualizations to study spatio-temporal data relating to thunderstorms. Unlike our tracking graph, they use a tracking graph with repeated node and edge crossings. Our work relates to the comparative visualization work by Alabi et al. [27], which showcases a visualization that uses opaque and transparent geometry. They introduce two sets of glyphs into the scene, which would add to the difficulty in perceiving differences in our context. In contrast, we do not use glyphs to show change in 3D as the visual clutter increases proportionally to the amount of deformations.

3. Requirement analysis

Based on discussions with experts, existing literature, and standard diagnostic protocols, we identified several important lesion attributes and potential approaches to visualize them. Although clinicians make use of 2D MRI slices for diagnosis, we found from the discussion with clinicians that there is a need for better interactive visual analysis tools, especially when studying lesion evolution in larger datasets for research purposes. The need for such supporting visualizations for longitudinal data arise mainly when dealing with a high number of follow-ups, high lesion load, and multiple modalities. According to a radiologist we interacted with, removing the manual effort that goes into comparing lesion pairs in the large longitudinal dataset is something that needs to be solved.

We conducted a requirement elicitation with the support of clinicians and subject experts for understanding the needs in longitudinal MS visualization. Even though we derive some of the primary motivations from existing literature, we carefully validated those requirements with clinicians as well. During requirement elicitation, we got an impression that more advanced tools are in particular of interest to researchers who are trying to decode the patterns in MS. The clinicians generally follow accepted and approved standards during clinical practice. Due to the fuzzy nature of the disease, whose underlying cause is still unknown, it was difficult for clinicians to comment on the exact application. We derived the high-level requirements based on the discussion with experts, including clinicians, whereas we derived the feature level requirements based on both literature and expert inputs.

Sugathan et al. [28] recently presented work on visualizing spatial aspects of lesions where the need for longitudinal MS visualization became clear. There is a significant manual effort to understand patterns from longitudinal datasets with large number of followups. Here, we see a requirement for better visualization approaches that can help in an explorative analysis of the entire range of longitudinal scan data for a subject. Besides visualizing statistical properties of lesions, we identify that it is

useful to see important events like the occurrence of new, enlarging, splitting, and merging lesions. In addition to capturing lesion volume-related features, we see a requirement for visualizing abnormalities in intensity related features, as they are useful in longitudinal studies [29]. We identify another requirement that is related to the complexity in understanding a 3D scene when there is a high lesion load. Unlike the existing tools, users would like to interactively analyze lesions without occlusion. Based on a discussion with a radiologist, we also found that, in some cases, it would be ideal to compare scans from arbitrary time points. According to the radiologist we interacted with, the normal comparison workflow always considers the current scan and previous scan. When analyzing follow-up data in a tool, it is useful to allow comparisons between arbitrary time points. As per the clinician, this would allow for them to capture the trend clearly.

Based on the requirement elicitation described above, we summarize the following main requirements:

- R.1 Visual support to quickly identify lesions of interest through exploratory analysis.
- R.2 Individual lesion changes in shape and extent over time must be shown.
- R.3 Lesion intensity changes over time should be shown for visual analysis.
- R.4 Detailed visualizations to study statistical lesion attributes in relation to new and enlarging lesions.
- R.5 A representation that supports understanding the state of lesions at the current time-point while having an overview of the whole time series evolution.

4. Longitudinal lesion visualization

To satisfy the requirements outlined in the previous section, we have designed and implemented a visualization application to support spatio-temporal lesion development analysis. An overview diagram of our visualization approach is visible in Fig. 5. We present all our interactive visualizations in an application written using Python and Qt. For data preprocessing, we use additional tools such as FreeSurfer and the Visualization Toolkit (VTK) and Insight Toolkit (ITK). After the preprocessing stages, our interactive visualization system can load longitudinal data of a single patient at a time.

We present the interactive visualizations using four dominant views as depicted in Fig. 5(c), (d), (e) and (f).

4.1. Preprocessing

Our visualization pipeline starts with a preprocessing module with structural MRI data along with annotations (binary lesion masks) as input. The reason for needing a preprocessing stage is due to dependency on FreeSurfer [30] for segmentation, which takes several hours to finish, and size of the longitudinal data. The application can handle both measured as well as simulated data sets. In this study, we have used a simulated dataset, which reflects a situation where there are many patient follow-up scans available to demonstrate the scalability of our approach to data with many followups and multiple modalities. The instances shown in Fig. 1 are from a real dataset that contains only a baseline and a single followup scan, which is less suitable for showcasing the potential of the application. Another motivation for using a synthetic dataset is that it enables us to mimic all possible morphological changes that a lesion can undergo. The synthetic dataset includes a total of 80 timepoints including the baseline. There are at most 8 lesions in each timepoint, and they undergo changes as already illustrated in Fig. 2. The real datasets when compared with our synthetic dataset, cannot expect many

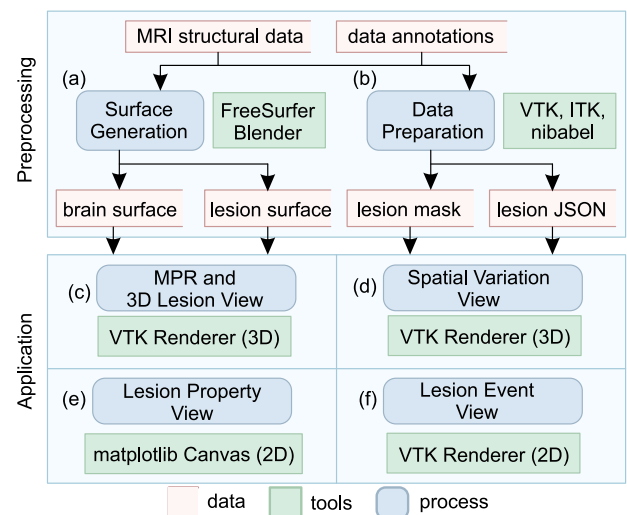


Fig. 5. An overview of our visualization system showing the components in the preprocessing and visualization stages. Preprocessing stage involves (a) surface generation and (b) preparing data using re-slicing and registration. The application finally provides interactive visualization through four different views ((c), (d), (e) and (f)) that are linked.

followups especially in a clinical setting. However, real datasets used in research studies that are aimed at exploring MS lesions can have many and frequent followups. We have developed this dataset in such a way that it gives clinicians or researchers an opportunity to consider the potential for clinical treatment assessment as well as research opportunities. When using a synthetic dataset, we avoid the need for volume registration of the data at all time steps by creating the synthetic data from the same original scan. When using real measured data, users can include a registration step using existing tools such as FSL [31], FreeSurfer Longitudinal [32,33] or Elastix [34]. Here we discuss some of the important preprocessing steps that need to be done before using the application:

4.1.1. Lesion surface and anatomy reconstruction

One of the first steps in the preprocessing module includes the extraction of lesion surfaces from volume data (Fig. 5(a)). In addition, when we display the resulting lesion mesh in the visualization tool, we also present context brain anatomy such as the cortical surface, ventricles, etc. This helps users to get spatial context while interacting with the lesions. To generate the surface of the brain and other subcortical structures, we use the standard FreeSurfer version 6.0 reconstruction pipeline. As shown in Fig. 5, our system considers the longitudinal structural scans and their corresponding data annotations (lesion masks) as mandatory inputs. When using a real dataset, we can extract lesion masks by employing manual or automatic segmentation. This can follow the use of any standard iso-surface generation algorithm for generating the lesion surfaces. Since we are using a synthetic dataset in the study, we create lesion surface profiles using the modeling capabilities available in Blender version 2.9 [35] and generate lesion masks from those surfaces. To mimic a corresponding change in the structural data, we also write varying intensities into the structural data at places where we created the synthetic lesions.

Besides lesions, we also need to display surfaces of other structures that can act as an anatomical context. For this, we obtain the brain surface from FreeSurfer reconstruction results and compute the ventricle surface from FreeSurfer segmentation results. In addition, we do necessary data transformations, volume reslicing,

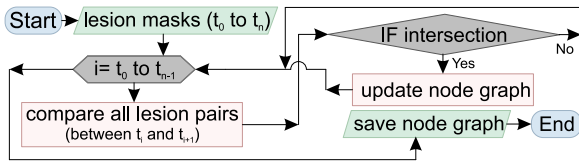


Fig. 6. High level flowchart for node graph generation.

and compute statistical information about lesions to reduce the computational overhead while running our application. We store part of the preprocessing results of the preprocessing as a JSON (JavaScript Object Notation) file. We configure the visualization application to use the data in the JSON file instead of processing the datasets for every user interaction.

4.1.2. Lesion tracking

To track a lesion between consecutive scans, we check for intersections between a pair of binary lesion masks and maintain a node graph to store the tracking information. Fig. 6 depicts the high level steps we use for the generation of a node graph. We keep this process in the preprocessing step because it is a time-consuming task which involves processing all the follow-up scan volumes. For tracking, we make use of the binary lesion mask volumes, where a scalar value of 1 represents lesion regions and a value of 0 represents non-lesion regions. Before our tracking algorithm, we label the mask volume lesions using connected component analysis. We cannot use the same lesion labels for tracking because it varies depending on the lesion shape and location inside the volume. To circumvent this problem, we use a separate graph-based data structure where the lesions are considered nodes and we store a time list and label list per node as node metadata. The directed edges of the graph reveal split or merge patterns and point toward the direction of advancing time. Algorithm 1 provides an overview of the lesion tracking script. In a nutshell, the algorithm traverses through all the labels in the dataset and iteratively builds a graph out of it. Every node in the graph represents a specific lesion, and every edge represents a split or merge event. Lesions that are not part of a splitting or merging event are represented by a single node. The lesion tracking data represented as a graph forms the basis for most of the computations and visualizations in our tool.

4.2. Visualization components

Before starting the visualization tool, we write all the preprocessed data from the previous step to folders with predefined names. We can assign a separate folder for every single subject and every subject folder can hold the individual follow-up scans. An overview of the visual components of our application can be seen in Fig. 7. In our application, we provide the commonly used Multiplanar reconstruction (MPR) images, which are the standard orthogonal planes (axial, coronal and sagittal) extracted from structural MRI data. For specifying lesions, we provide an overlay of the lesion mask on all the three MPRs. To provide extra guidance when a user interacts with 3D lesions, we automatically update the MPR planes to show the slices having the selected lesion. In addition to the standard MPR view available in many clinical applications, we provide four views representing additional visual encoding and functionality to support task in longitudinal lesion data analysis.

Algorithm 1: Lesion tracking for longitudinal MS data

Data: S , an array storing scan data of a subject.
Result: G , a directed graph storing lesion tracking data.

```

1  $N_S \leftarrow n(S)$ ; /* Number of follow-ups */
2  $N_0 \leftarrow$  number of lesions in  $S_0$ ; /* baseline */
3 Initialize  $G \leftarrow$  graph with  $N_0$  disconnected nodes;
4 for  $i = 1$  to  $N_S$  do
5    $p \leftarrow$  Set of lesions in  $S_{i-1}$ ; /* previous scan */
6    $q \leftarrow$  Set of lesions in  $S_i$ ; /* current scan */
7    $N_p \leftarrow n(p)$ ; /* #Lesions (previous) */
8    $N_q \leftarrow n(q)$ ; /* #lesions (current) */
9   Initialize  $pData \leftarrow NULL$ ;  $qData \leftarrow NULL$ ;
10  for  $j = 0$  to  $N_q$  do
11    for  $k = 0$  to  $N_p$  do
12       $pData \leftarrow$  Append intersection  $p_k$  on  $q_j$ ;
13       $qData \leftarrow$  Append intersection  $q_j$  on  $p_k$ ;
14    end
15  end
16  for  $k = 0$  to  $N_q$  do
17    if  $qData_k$  has intersection then
18      if multiple intersection then
19        Add new node in  $G$  and set metadata;
20        Add edge between relevant nodes in  $G$ ;
21      else
22        Update metadata of existing node in  $G$ ;
23      end
24    else
25      Add new node in  $G$ ;
26    end
27  end
28  for  $k = 0$  to  $N_x$  do
29    if  $pData_k$  has multiple intersection then
30      Add edge between relevant nodes in  $G$ ;
31    end
32  end
33 end
  
```

4.2.1. 3D lesion view

To support requirement R.1, we use lesion surfaces as an interactive object and render them in spatial context to brain anatomy. Fig. 7(f) shows the 3D visualization of lesions along with minimal context information that helps users to get an impression of the overall lesion load and distribution. The 3D lesion view basically renders all the lesions along with the ventricles inside the brain, and acts as the primary view where user interaction typically starts. A common method to provide context involves supporting user interaction on the image planes (MPRs) itself, but it is challenging to get a full picture of the lesion development over time across multiple imaging sequences due to multiplane navigation and the mental load of constructing a 3D view from 2D slice information. As an alternative, we provide the visualization as a 3D scene where we can also render other 3D structures, such as the ventricles, to provide spatial context. The lesion surface data is available from the lesion mask data while the ventricle surface can be acquired from segmentation in, for example, FreeSurfer. We choose ventricles as a context structure instead of the brain surface to provide an occlusion-free view of the lesions. Using the ventricles as a context also helps us to assess radiographic features such as Dawson fingers [36], i.e., a situation where lesions appear in a specific pattern near the ventricles. The view also includes a standard orientation marker to provide a correct impression of brain orientation.

We use the same viewport for displaying a comparative visualization of lesions. Here, we inspire the conceptual design of the visualization based on the inputs we received from a radiologist. According to the radiologist, the usual clinical workflow compares a scan with its immediate previous scan. Instead of this, it is sometimes useful to compare two arbitrary timepoints for studying long-term trends especially in longitudinally large datasets. Here, if the user-selected duration is large, then we can expect significant changes in shape and spatial distribution of lesions.

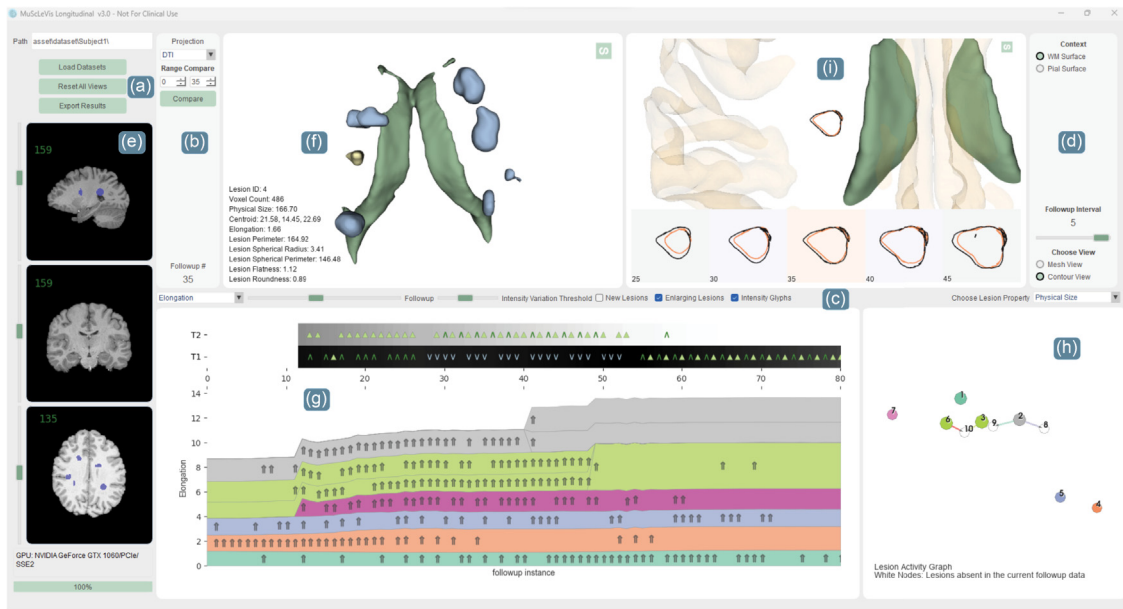


Fig. 7. Our system for explorative analysis of MS longitudinal lesions. The application consists of main user interface controls (a,b,c,d), MPR views (e), 3D lesion visualization (f), stack plot and intensity plots (g), node graph visualization (h), and visualization for longitudinal shape analysis for a selected lesion (i). The linked visualization views (f,g,h,i) help to perform interactive analysis on longitudinal lesion research data.

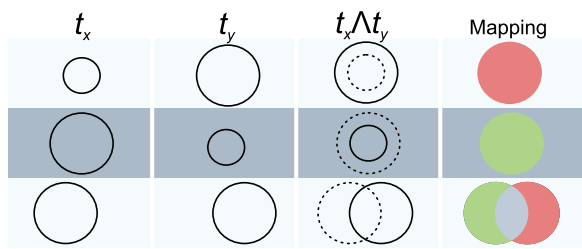


Fig. 8. Comparative visualization of abstract lesion differences computed between an arbitrary range of time points, t_x and t_y where $x < y$. In the third column showing the combination of two surfaces, we represent the lesions from time point t_x and t_y using dotted and solid curves, respectively. When color mapped, we use a red-like color to show areas where a lesion is growing, green-like color to show areas where lesion is shrinking, and a gray color to show areas without change.

This significant difference makes a glyph-based visualization a poor choice for conveying change information. By displaying a combination of surfaces from both timepoints as a single surface enables us to mark (using color patches) the areas where the lesion is improving (shrink) and the areas where the lesion is getting worse (grow). Even though the combined surface can sometimes include mesh fragments from both timepoints, it gives useful information on the change pattern of the lesions. The size and location (on the lesions) of the color patches gives a high level information on the degree of MS activity. As shown in Fig. 8, we compute the visualization for an arbitrary range of time points t_x and t_y , set by the user. We generate a combined mask volume M and a corresponding mesh M_s , from time points t_x and t_y to visualize lesion changes. For probing purposes, we generate a difference volume D that stores the difference values (representing growth, shrinkage or no change) between the original lesion meshes at time points t_x and t_y . To copy the difference values to M_s , we probe M_s on D . We then enable the scalar-based coloring for the mesh M_s , where vertices with scalar values less than zero, equal to zero, and greater than zero get the color values red, gray, and green, respectively. Please note that the colors are not pure red and green, but colorblind safe shades from ColorBrewer [37]. We

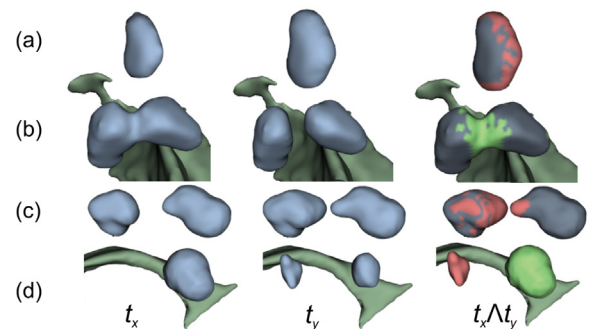


Fig. 9. Example visualizations showing specific lesion change patterns for a set of lesions captured from time points t_x and t_y . (a) A lesion growing only towards a certain direction. (b) a lesion splitting into two separate lesions, (c) two lesions growing towards each other, and (d) two lesions where one of them shrink and the other appear as new.

use these colors to communicate the improving and worsening lesions.

The visualization shown in Fig. 9 captures some example patterns from the range compare visualization. In the figure, the first two rows represent the inputs from time points t_x and t_y . The last row represents the resulting visualization that shows the color mapped lesions. We show the change pattern using red, green, and gray colors representing growing, shrinking, and inactive parts of lesions, respectively. In Fig. 9(a), we show a visualization that identifies lesion growth in a specific direction. This visualization can be used to study whether a lesion is growing towards a specific structure or not. Fig. 9(b) captures the splitting location of a lesion and 9(c) shows a merging lesion when comparing the data from time steps t_x and t_y . If there are significant uniform variations all around the surface of a lesion, we would get a similar visualization as shown in Fig. 9(d).

4.2.2. Lesion property view

To visualize the different statistical lesion properties, we consider a stack plot as the basis for encoding lesion information.

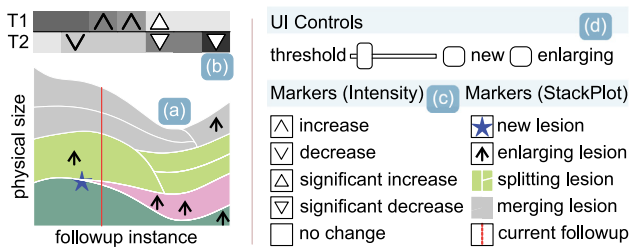


Fig. 10. An abstract depiction of stack plot design for showing lesion features such as physical size evolving over time with each lesion encoded in a color (a). Abstract depiction of intensity visualization highlighting individual lesion properties and their changes over time (b). To convey additional information, we overlay different markers (c) that can be manipulated using the user interface controls (d).

This view fulfills requirement R.1, R.3 and R.4. In our application, we render the stack plot as shown in Fig. 7(g). An illustration of the stack plot design and related aspects is shown in Fig. 10. The motivation for using a stack plot comes from the limitations in extending the visualizations depicted in Fig. 3. In addition, the changes happening to the total lesion volume load is better understood when using a stackplot than using a bar chart visualization. With our design choice, a user can easily track the changes of a single lesion over time, while conveying the overall trend of lesion load. For instance, if we consider the depiction in Fig. 10(a), we can see that the lesion represented as a pink-colored stackplot component undergoes enlargement while the total lesion load reduces. The parallel observations on individual lesions and overall lesion trend is useful to identify lesions that are deviating from a global trend. For the stack plot, we use colors from ColorBrewer [37] that are color-blind safe. The color coding makes it easier to identify a lesion across multiple visualizations in the application. By using different colors and adding borders for stack plot components, we can easily understand relative sizes of individual lesions and the events like merging, splitting and appearance of new lesions. It is important to note that we visualize the longitudinal lesion data in such a way that the lesions linked to the same event are ordered together in the stack plot and get the same color. Understanding total lesion volume load from the stack plot is a useful aspect for clinicians because it can show whether a patient is improving or not in relation to treatment. In the stack plot, we plot the follow-up instance on the x-axis and a user set lesion property on the y-axis. Lesion volume is the most useful and default feature we assign to the y-axis. It is possible to change the y-axis variable to any other available statistical feature as needed.

For a selected lesion in the stack plot, we display the average voxel intensity visualization in a plot as shown in Fig. 10(b). We present the intensity information in a way that supports comparison across modalities and time. We always show the grayscale intensities of a pair of modalities in the intensity plot. In Fig. 10(b), the modality T1 follows an increasing pattern of voxel intensity and T2 shows a decreasing pattern. With the intensity visualization, we intend to support researchers who study or model intensity variations.

Unlike regular stack plots that plot the data arrays in arbitrary order, we sort the data such that lesions that are connected by events such as merge or split comes together. To derive this order for the stack plot data arrays, we rely on a graph G , which captures the split/merge events that may occur during the lesion timeline. In G , we consider any of its subgraphs with a minimum 3 nodes as a case of a split or a merge event. We plot the stack plot in such a way that all the nodes corresponding to a split or merge event are aligned as much as possible by their vertical ordering.

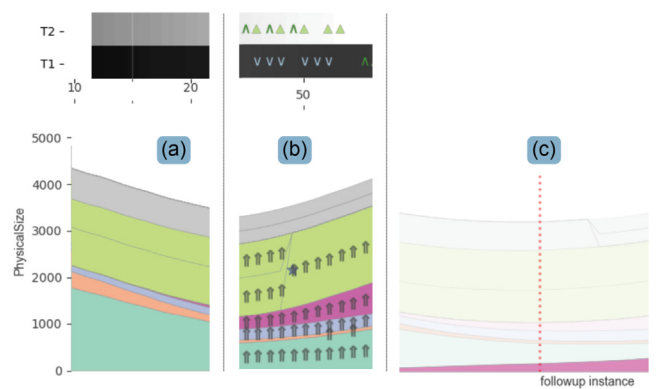


Fig. 11. The stack plot and intensity plot show lesion evolution over time. The state of the plots without overlay markers (a) and with overlay markers (b). By right clicking on a specific lesion (pink), the user can bring a specific lesion plotted over a flat baseline (c).

We overlay several markers shown in the first column of Fig. 10(b) on the intensity visualization plot. These markers indicate the degree of intensity changes between consecutive time points t_x and t_y where $y \neq 0$. If there is no intensity difference between consecutive time points, no markers will be shown. The second column of markers in Fig. 10(b) shows the markers used on the stack plot. Based on the user requirements, we also provide user controls (Fig. 10(d)) that determine the computation and appearance of the glyphs.

Fig. 11 shows three example screenshots with different states of the stack plot visualization. During application development, with the help of an experienced radiologist, we refined the design of the stack plot. Initially, the intensity visualization and overlay glyphs were separate views from the stack plot. Based on the inputs received in a feedback discussion, we synchronized the intensity visualization with the stack plot, and added glyphs as an overlay on top of the stack plot. According to the radiologist, bringing everything into one place is more useful than separating them for the sake of avoiding clutter. This is the reason we provide options to enable/disable overlay glyphs.

4.2.3. Lesion event view

For an overview of events that happen during lesion evolution over time, we provide an interactive node graph visualization in addition to the stack plot. An illustrative example depiction of such a node graph is shown in Fig. 12. Fig. 7(h) shows an example render of the node graph in our application. In the node graph, every node represents a unique lesion and the directed edges represent either a split or merge scenario of lesion(s). The arrows in the graph point to the direction of time advancement, where the origin of the arrow points to a lesion which was subsequently merged or split. The entire node graph visually communicates lesion information representing all the time points, while showing indications of currently active lesions for a specific time point. This fulfills requirement R.1 and R.5. Nodes that are colored in white show lesions that are absent in the currently selected time point or follow-up instance. Colored lesions in the graph represent the present lesions in the current follow-up. The colors correspond to the colors in the stack plot for visual linking. To visualize the statistical properties of the lesions, we support encoding several lesion properties as graph node sizes. With this, we link the node graph with other views, especially when there are too many tiny lesions to get a good overview or when there is a high variance in the physical size of the lesions. In the latter case, the larger lesions will dominate the stack plot and it is possible

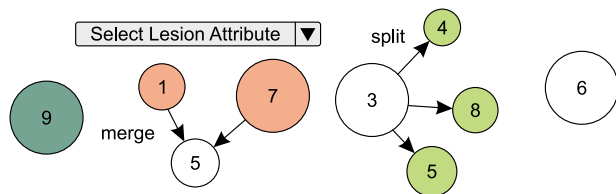


Fig. 12. The node graph view displays a summary of lesion event data and selected lesion properties. The drop down box allows for statistical lesion parameters to be mapped to node size.

that one may overlook the small lesion events. We update the node graph visualization whenever the user interacts with the time slider. We also see lesion properties (set using a combo box) encoded as the size, i.e. circle radius, of the nodes in the node graph. The nodes will always keep a default minimum size for proper visibility. To map lesion attributes to nodes, we add the normalized lesion attribute values to the default node sizes. We can see value and topological changes as an animation by updating the current time using the time slider. In contrast to the stack plot, sometimes the node graph can serve as a better alternative for understanding lesion events. This is true especially when we have tiny lesions and high lesion load for a dataset. The linking between stack plot and node graph helps a user to refine the observations obtained from the visualizations.

4.2.4. Spatial variation view

Both the stack plot and the node graph focus on conveying change information purely based on the statistical properties of lesions. To support requirement R.2, we provide the 3D spatial variation visualization, where we aim to provide multiple (past, current and future) comparisons performed around a selected time point for a selected lesion. With this view (Fig. 7(i)), occluding lesions are less of a concern, as the user explores only one selected lesion at a time. Selectively displaying lesions like this, along with local context information, helps a user to understand shape changes in relation to other brain structures. When a selected lesion undergoes a split, merge, or disappear event, the selection highlight will disappear and the lesion viewport stops updating. These major events are also visible from the color changes in the node graph.

We designed our visual encoding to support exploratory analysis of the spatial activity trend of a single lesion. A high level design depiction of the viewport setup for studying spatial variation is given in Fig. 13. The module contains six viewports. The main viewport (see Fig. 13(a)) is at the top, and we reserve it for displaying the selected lesion along with brain context structures. For anatomical context, we display the ventricles and a transparent brain surface rendering. To display longitudinal lesion changes, we use the remaining five viewports at the bottom, inspired by motion animation sequences (see Fig. 13(b), (c), (d), (e), and (f)). Among those five lesion viewports, the middle viewport renders the current lesion, and the viewports spanning to the left and right, displays the previous and future timepoints, respectively. By default, the viewports at the bottom render a contour view of a selected lesion based on the viewing angle. Since a side-by-side visualization of the data from two time points is not ideal for perceiving spatial differences, we also display the contour from the previous time point as an overlay. As shown in the lesion viewports in Fig. 13, the black color contour in a particular viewport represents a lesion from the time point displayed in the same viewport. In every lesion viewport, we use an orange contour to represent a lesion coming from a previous time point. As shown in Fig. 13, the contour view can convey

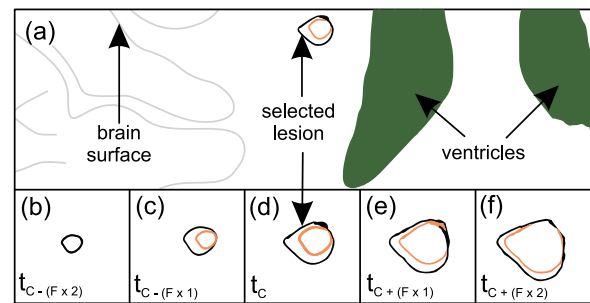


Fig. 13. Design for the analysis of spatial changes of individual lesions. Here, we use (a) a context viewport to display the selected lesion relative to other brain structures. The views (b), (c), (d), (e) and (f) represent lesion viewports, where we render lesions with an overlay from one of the previous time points.

the spatial difference in contours when looking from the viewer's perspective. This helps a user to align the brain context shown in Fig. 13(a) to a suitable orientation where we can study relevant changes in the lesion. Having the contour visualization along with a linked brain context enables a user to understand whether a lesion is active toward a specific anatomy or not. The user can also switch to a mesh view to see the lesion difference in 3D. Here, instead of a combination of black and red, we use blue and orange colors, respectively. If a previous time point is not available, we do not show the orange contour as shown in Fig. 13(b).

We use a follow-up interval value, F to determine which previous and next time points to display. The value F is user adjustable. Consider a dataset with several time points. If a user wants to study a specific time point, say C , by using a follow-up interval value F , then selecting a lesion at time point t_C would display lesions from the time points; $t_{C-(F \times 2)}$, $t_{C-(F \times 1)}$, t_C , $t_{C+(F \times 1)}$ and $t_{C+(F \times 2)}$. For the overlay, the viewports would use the time points $t_{C-(F \times 3)}$, $t_{C-(F \times 2)}$, $t_{C-(F \times 1)}$, t_C , and $t_{C+(F \times 1)}$. We show an example of the visualization outcome for different values of the follow-up interval in Fig. 15. As the follow-up interval increases, changes become more pronounced. A suitable value for the follow-up interval purely depends on the degree of lesion changes and may vary across patients. When increasing the zoom level, it is possible to see the volumetric differences as shown in Fig. 15(b). When we zoom out, as shown in Fig. 15(c), we do not see the details but an abstract view of mesh variations. This gives us an abstract view of mesh variations. In terms of workflow, a user can first inspect the 3D lesion zoomed out, and then later start looking at the details by zooming in. Since the appearance of new lesion is clinically important, we visualize them in the stack plot with an additional glyph.

We choose to include a contour visualization in the design to help understand the direction of lesion activity towards certain brain structures. To quote an example scenario, imagine that there is a lesion near the optical nerve; if the lesion grows toward the optical nerve, then it is more likely that the patient may experience vision problems in the future. For comparing two lesions using the mesh view, we use a design where we render both the lesion meshes together with different styles (surface and wireframe) in the same space as this helps to identify surface areas where the one lesion changes compared to the other. In our design, we use five lesion viewports because showing consecutive pairs of lesions is useful to understand the trend of spatial variation, inspired by the current clinical practice of comparing two scans at a time.

4.3. Interaction and linking

To support exploratory analysis studies on lesions, we structure our visualization idioms as multiple linked views. Here,

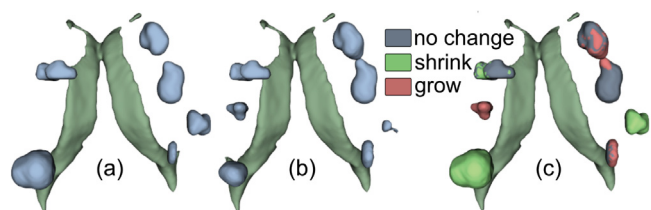


Fig. 14. Comparative visualization of lesions at two arbitrary time points (a) x and (b) y where $x < y$. The user can toggle between lesions at current time step y and (c) an abstract change visualization depicting the lesion changes using different colors.

we discuss all interaction- and linking-related aspects that are integrated in our visualizations. To visually understand the main interactions in the application, please refer to the supplementary video accompanying this paper.

3D lesion view: This view is intended to be the starting point for analysis. A mouse selection of a lesion in this view will highlight the lesion and also show statistical properties as a text overlay. Using the time slider, we can visually inspect the changes happening to the surface mesh and properties of the selected lesion. The surface mesh changes appear as an animation, which is useful to capture the nature of the changes happening. We link this view to other view on-demand based on whether the Control key is pressed on the keyboard.

Since we use the same viewport for providing the range compare visualization, we can exploit the benefits of toggling between original lesion view (Fig. 14(b)) and the comparison view (Fig. 14(c)). While the comparison view conveys abstract information about lesion changes, toggling to the original lesion view can help users to assess the amount of difference that happened to the lesions.

Stack plot and intensity visualization: We provide user-selectable components in the stack plot to relate observations with other views. The glyphs we display on the intensity plot depend on the value set by the intensity variation threshold slider provided in the user interface. We can dynamically set the threshold value and it defines the amount of variation above which the intensity change is significant. The stack-plot can also display glyphs showing new and enlarged lesions. In terms of design, we implemented this as an on-demand feature to minimize clutter. Even though the stack plot provides an excellent overview of the lesion load trends over time, it might be difficult to understand the size variation happening to individual lesions. This happens as many components get plotted on a curved x -axis baseline. Except for the bottom component, which gets plotted on a zero x -axis baseline, all the remaining components in the stack plot usually get plotted on a non-straight baseline. To help users get a good understanding of the lesion size difference, we provide an option to pick the stack plot components using the right mouse click. This interaction will plot the selected component on a zero x -axis baseline as a temporary overlay. By default, we use a scale-to-width display style for plotting the stack plot inside the viewport. Here, if there are too many follow-ups in the dataset, reading the intensity visualization horizontally would be difficult, especially when there are active glyph overlays. To remedy this, we have enabled a zoom and pan interaction using the mouse scroll wheel to provide a detailed view of intensity changes as needed. Since we have linked the x -axis of the stack plot and the intensity plot, interaction on the stack plot will also proportionally affect the intensity visualization. Keeping the x -axis of both the visualization in sync also helps us to compare and analyze data vertically.

Node-graph visualization: The link between the node graph and the stack plot is useful especially when the stack plot contains a lot of information due to high lesion load. The need to spot tiny lesions also motivated the design of the node graph. Interaction with the nodes will show the relevant components in the stack plot and highlight corresponding lesions in the 3D lesion view. Using a rectangle selection, users can also select multiple items from the node graph and can find related items in the stack plot.

Spatial change visualization: For a selected lesion in the 3D lesions view, we visualize detailed spatial variations in the lesion viewports. The time slider at this point will remain linked with this view as long as there is tracking information available. This linking enables us to inspect the shape evolution of the selected lesion at any time point. The linking between context viewports and lesion viewports is unidirectional. Any interaction on the lesion viewports will update the contents in the context viewport due to the view synchronization, but no interactions in the context viewport will disturb the lesion viewport. We use this design because the context is a view that supports the lesion viewports. Interactions in the context view by rotating in 3D are useful for inspecting the lesion surroundings for a specific visualization/feature found in the lesion viewport. We added the follow-up-interval control based on the input of a radiologist, who wanted to see trends better by increasing the followup duration.

5. Evaluation

We conducted a qualitative user study to assess the utility and potential for impact of the visualizations and application we developed.

5.1. Evaluation setup

The user study was set up to understand the usefulness of the application from a clinical and medical research perspective, and our participant pool aligns with this background. We include four experts with relevant knowledge and experience in brain research. Among the four participants, there are two experienced radiologists who helped us to understand the utility of the application from a clinical perspective. To assess the utility for the research community, we also included two additional participants with backgrounds in brain and MS research. We followed these general steps for both onsite and remote study participants:

1. We made the participants aware of the features available in existing tools through a presentation.
2. We demonstrated the tool to the experts by giving a walk-through of all the important features in a live demo.
3. We let the participants interact with the tool and encouraged them to think-aloud.
4. We captured additional feedback about the visualizations using a prepared set of statements.

In the user study, we allowed the users to interact with our tool after providing them a feature demonstration. For the questionnaire part, we asked the users to submit their responses on a five-point Likert scale with possible answers: Strongly Disagree, Disagree, Neutral, Agree and Strongly Agree. The questions were phrased in a way that 50% of them take a negative form to reduce bias. All the 18 statements are included in Table 1. Negative statements are marked with an asterisk and phrased positively with inverted scores for ease of interpretation.

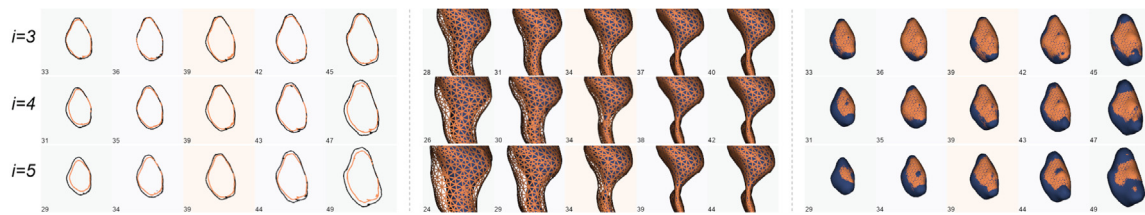


Fig. 15. Example visualization results from the spatial variation view for different follow-up interval values $i = 3$ to 5. (a) A contour visualization for a user selected lesion, (b) a mesh visualization (when zoomed in) showing longitudinal lesion evolution where zooming in helps a user to see volume differences, and (c) a mesh visualization (when zoomed out) showing longitudinal lesion evolution where zooming out provides a better abstract perception of lesion changes.

5.2. Evaluation results

The first participant C1 is an experienced clinician with 7 years of experience in radiology. The second participant C2 is also an experienced clinician having 11 years of experience in radiology. To better understand the research utility, we included participants R1 and R2 with a background in brain research.

Thinking about the potential users, C1 stated that the tool can be useful for clinical experts and that the usage is not limited to the research domain. The user C2 being well aware of the standard criteria for reading MS lesions from MRI slices, stated that the tool can have several potential research benefits. Overall, C2 agrees with the potential utility of the application. Participant R1, having experience with MS lesion research, commented that the tool has great potential to find useful patterns in longitudinal MS data. R2, who has experience in using several research tools, commented that the user interface of the tool is excellent when compared to other similar research tools. After interacting with the application, R2 left some additional comments stating that the range of analysis tools was impressive and the user interface was enjoyable. R2 also finds that the application's performance is fast, especially for the user interactions. Finally, R2 appreciated the detailed measurement variations presented in the application.

We had some areas in the application where the users provided some negative feedback. In the user study feedback form, C1 commented that besides the glyphs, it would be nice to have relative differences provided in numerical form. C2 was not sure about the benefit of the node graph because C2 could not find a clinical use case. However, C2 stated that the node graph might be useful for researchers who deal with large and complex datasets. While adding responses in the feedback form, C2 commented that the responses are purely based on standard radiology workflows and do not consider any research users. In general, C2 disagreed with all the statements (3, 4 and 15) relating to the node graph. In addition, C2 did not like the original glyphs we used in the stack plot. At the time of the user study, we had tiny circles showing enlarging lesions. C2 said that the response would go in favor of the application if we changed the circular glyph to an arrow pointing upwards. Based on C2's preference, we revised relevant visualizations to use an arrow glyph. With this revision, we addressed the negative comment about the overlay glyph. Apart from this, thinking from a clinical perspective, C2 remained neutral for statements 8 and 14 because C2 could not relate to any direct clinical uses.

Overall, the users from a research background consider our visualizations to be beneficial with no negative responses to the user study statements.

6. Discussion

The evaluation results show that there is a good degree of agreement on the utility of the application. The visualization results generated based on lesion change patterns in the synthetic

dataset were sufficient to convey the potential. In particular, the stack plot visualization synced with multimodal intensity visualization received good feedback due to its capability to convey the trend of total lesion load while showing individual lesion states. With added interactions and overlays, the module received the most attention. One limitation we see with the stack plot is the increased interaction effort when there are many tiny lesions present in the dataset. In such scenarios, a user will have to zoom-in and/or pan for exploring lesions. In our synthetic dataset, we prioritized covering all possible morphological lesion changes. To handle scenarios where there are many tiny lesions, we anticipate increased use of the node graph visualization as a better medium to understand the lesion properties and events. The linking between the views enables us to relate the identified features or patterns.

When compared with existing tools discussed in Section 2, our visualizations are more effective according to the users we had in the evaluation. In contrast to the bar chart-based visualization shown in Fig. 3, we found that the stack plot is a more scalable approach that does not compromise the user's ability to comprehend the nature of the longitudinal dataset.

The visualization pipeline visible in Fig. 5 will have to incorporate registration steps using external libraries or make use of the FreeSurfer capabilities for measured datasets. When considering the range-compare visualization, by using a synthetic dataset, we benefit from perfect registration, which we visualize as areas of no change. On a real dataset, we foresee the inclusion of some tolerance in the probing mechanism to correct for imperfect registration and partial volume effects. It is important to note that while the synthetic dataset mimics all the lesion shape variations that are possible, it does not mimic any pathology specific features such as activity rate, activity distribution and specific spatial distribution patterns of lesions, as we may observe in a real dataset. If we consider deployment of this tool, it is a limitation that the application depends on the time-consuming FreeSurfer preprocessing. The delay in preprocessing further increase for real datasets because of the dependency on medical image registration.

It was a bit difficult to do the design research solely from clinician inputs. This was mainly because the clinicians were more used to 2D than 3D. In order to convey the potential of better visualizations for longitudinal studies, we found it useful to show existing visualizations from the literature. This helped the radiographer to comment on what would be useful, and guide our visualizations to maximize potential benefits. Considering the reusability of our visualizations, we also emphasize that it is feasible to generalize our visualization application to handle other kinds of pathologies, such as a brain tumor analysis. In summary, while the synthetic data highlights the scalability of our approach, clinical use cases for real datasets and optimization of the preprocessing workflow need to be investigated in more detail.

Table 1

User response to 18 statements on a 5-point Likert-scale: 1: Strongly disagree, 2: Disagree, 3: Neither agree nor disagree, 4: Agree, 5: Strongly agree. Negatively phrased statements in the original form are indicated by a * . Their phrasing and scores are inverted for ease of interpretation.

Statement	C1	C2	R1	R2
1 The visualization tool is useful for explorative analysis of longitudinal MS lesions *	5	4	4	5
2 It is useful to have an interactive stack plot for studying the progression of MS lesion features (especially the volume of lesions) *	5	5	4	5
3 MS lesion activity presented in the interactive node-graphs helps to get an easy summary of events like split, merge, and appearance of new lesions *	4	2	5	5
4 The node graph provides a good overview of the total number of lesions across timepoints *	4	2	4	5
5 The support offered by the application to pick individual lesions and study the changes while comparing with previous scans is useful	5	4	5	5
6 Selecting individual lesion data from the stack plot and relating it with other visualizations is NOT helpful *	5	4	5	5
7 Showing new lesion indicators in the stack plot is a useful feature when exploring datasets with tiny lesions & high lesion load *	4	4	5	5
8 Horizontally visualizing the intensity of a selected lesion for multiple modality and follow-up helps *	4	3	4	5
9 Showing lesion properties as glyph overlays on intensity visualization is helping to understand the increase/decrease trend of a lesion under study	4	4	5	5
10 While interactively selecting lesions from the stack plot using the right mouse button, display of individual lesion data on a zero-baseline helps me to read the longitudinal progress clearly *	4	4	4	5
11 The slider control provided for traversing through all the time points while viewing immediate updates on other views (stack plot, node graph and lesion overlay timeline) is useful	5	5	5	5
12 Display of individual lesions with detailed contour and surface differences while having a linked view to the brain context is useful	4	4	5	5
13 The contour visualization helps me to see the volume changes from the view perspective	5	5	4	5
14 Displaying the current and previous time point lesions as surface and wireframe respectively is a good choice to get an idea about the spatial differences of both lesions	5	3	5	5
15 The statistical properties of lesions encoded as node sizes in the node graph is useful	4	2	4	5
16 Visualizing the changes in an abstract form using the “Range Compare” feature is NOT useful *	4	4	5	5
17 Using the Ctrl+right click action on views for on-demand linking with other views is useful	4	5	4	4
18 Visualizing longitudinal landmarks to indicate enlarging lesions (overlaid on the stack plot) is useful *	5	2	5	4

7. Conclusion and future work

We have presented a visualization tool composed of multiple linked visualizations tailored for supporting explorative studies on longitudinal MS data. The user study participants helped us discover the utility of the tool in understanding overall lesion trend, individual lesion patterns, and in the possibility of inferring new findings through lesion research. We performed the evaluation using a synthetic dataset that only mimics the lesion shape and intensity variations. However, this did not affect the understanding of the potential uses of the visualization design. We also emphasize the interactive linking we enabled between our detailed visualizations and a real 3D brain context which is familiar to clinicians, which became a main reason for the acceptance by the radiologists.

For a better adaptability of this tool in lesion research, we see that further directions in our work include automating preprocessing pipelines enabling researchers to integrate this tool to their existing data pipelines. This step will bring the tool closer to a clinical and research audience alike.

CRedit authorship contribution statement

Sherin Sugathan: Conceptualization, Methodology, Software, Visualization. **Hauke Bartsch:** Resources. **Frank Riemer:** Resources. **Renate Grüner:** Resources. **Kai Lawonn:** Supervision. **Noeska Smit:** Supervision, Writing – review & editing, Funding acquisition.

Declaration of competing interest

The authors declare the following financial interests/personal relationships which may be considered as potential competing interests: Noeska Smit reports financial support was provided by Trond Mohn Foundation. Renate Gruner reports financial support was provided by Carl-Zeiss Foundation.

Data availability

Data will be made available on request.

Acknowledgments

This work was partially funded by the Trond Mohn Foundation (grant number 811255 and 813558) and the Carl-Zeiss Foundation.

Appendix A. Application demonstration video

Supplementary material related to this article can be found online at <https://doi.org/10.1016/j.cag.2022.07.023>.

References

- [1] Dobson R, Giovannoni G. Multiple sclerosis – a review. *Eur J Neurol* 2019;26:27–40. <http://dx.doi.org/10.1111/ene.13819>.
- [2] Bushnik T. Expanded disability status scale. In: Encyclopedia of clinical neuropsychology. Springer New York; 2011, p. 997–9. http://dx.doi.org/10.1007/978-0-387-79948-3_1805.
- [3] Vrenken H, Jenkinson M, Horsfield MA, Battaglini M, Schijndel RAV, Rostrup E, Geurts JJ, Fisher E, Zijdenbos A, Ashburner J, Miller DH, Filippi M, Fazekas F, Rovaris M, Rovira A, Barkhof F, Stefano ND. Recommendations to improve imaging and analysis of brain lesion load and atrophy in longitudinal studies of multiple sclerosis. *J Neurol* 2013;260:2458–71. <http://dx.doi.org/10.1007/s00415-012-6762-5>.
- [4] Thompson AJ, Banwell BL, Barkhof F, Carroll WM, Coetzee T, Comi G, Correale J, Fazekas F, Filippi M, Freedman MS, Fujihara K, Galetta SL, Hartung HP, Kappos L, Lublin FD, Marrie RA, Miller AE, Miller DH, Montalban X, Mowry EM, Sorensen PS, Tintoré M, Traboulsee AL, Trojano M, Uitdehaag BMJ, Vukusic S, Waubant E, Weinshenker BG, Reingold SC, Cohen JA. Diagnosis of multiple sclerosis: 2017 revisions of the McDonald criteria. *Lancet Neurol* 2018;17(2):162–73. [http://dx.doi.org/10.1016/S1474-4422\(17\)30470-2](http://dx.doi.org/10.1016/S1474-4422(17)30470-2).
- [5] Zhang Y, Chanana K, Dunne C. IDMVIS: TEmporal event sequence visualization for type 1 diabetes treatment decision support. *IEEE Trans Vis Comput Graph* 2019;25(1):512–22. <http://dx.doi.org/10.1109/tvcg.2018.2865076>.
- [6] Lawonn K, Smit N, Bühler K, Preim B. A survey on multimodal medical data visualization. *Comput Graph Forum* 2017;37(1):413–38. <http://dx.doi.org/10.1111/cgf.13306>.

- [7] Raidou R, van der Heide U, Dinh C, Ghobadi G, Kallehauge J, Breeuwer M, Vilanova A. Visual analytics for the exploration of tumor tissue characterization. *Comput Graph Forum* 2015;34(3):11–20. <http://dx.doi.org/10.1111/cgf.12613>.
- [8] Mainero C, Granberg T. Visualization of cortical MS lesions with MRI need not be further improved – NO. *Multiple Scler J* 2016;23(1):17–9. <http://dx.doi.org/10.1177/1352458516666336>.
- [9] Okuda DT, Moog TM, McCreary M, Bachand JN, Wilson A, Wright K, Winkler MD, Ramos OG, Blinn AP, Wang Y, Stanley T, Pinho MC, Newton BD, Guo X. Utility of shape evolution and displacement in the classification of chronic multiple sclerosis lesions. *Sci Rep* 2020;10:1–8. <http://dx.doi.org/10.1038/s41598-020-76420-8>.
- [10] Xin B, Huang J, Zhang L, Zheng C, Zhou Y, Lu J, Wang X. Dynamic topology analysis for spatial patterns of multifocal lesions on MRI. *Med Image Anal* 2022;76:102267. <http://dx.doi.org/10.1016/j.media.2021.102267>.
- [11] ao Fartaria MJ, Kober T, Granziera C, Cuadra MB. Longitudinal analysis of white matter and cortical lesions in multiple sclerosis. *NeuroImage: Clin* 2019;23:101938. <http://dx.doi.org/10.1016/j.nicl.2019.101938>.
- [12] Kuckertz S, Weiler F, Matusche B, Lukas C, Spies L, Klein J, Heldmann S. A system for fully automated monitoring of lesion evolution over time in multiple sclerosis. In: Drukker K, Mazurowski MA, editors. *Medical imaging 2021: computer-aided diagnosis*. SPIE; 2021. <http://dx.doi.org/10.1117/12.2582156>.
- [13] Tory MK, Moeller T, Atkins MS. Visualization of time-varying MRI data for MS lesion analysis. 4319, 2001, p. 590–8. <http://dx.doi.org/10.1117/12.428104>.
- [14] Köhler C, Wahl H, Ziemssen T, Linn J, Kitzler HH. Exploring individual multiple sclerosis lesion volume change over time: Development of an algorithm for the analyses of longitudinal quantitative MRI measures. *NeuroImage: Clin* 2019;21:101623. <http://dx.doi.org/10.1016/j.nicl.2018.101623>.
- [15] Filippi M, Rocca MA, Horsfield M, Comi G. A one year study of new lesions in multiple sclerosis using monthly gadolinium enhanced MRI: Correlations with changes of T2 and magnetization transfer lesion loads. *J Neurol Sci* 1998;158(2):203–8. [http://dx.doi.org/10.1016/s0022-510x\(98\)00126-9](http://dx.doi.org/10.1016/s0022-510x(98)00126-9).
- [16] Brune S, Hgestl EA, Cengija V, Berg-Hansen P, Sowa P, Nygaard GO, Harbo HF, Beyer MK. LesionQuant for assessment of MRI in multiple sclerosis—A promising supplement to the visual scan inspection. *Front Neurol* 2020;11:1700. <http://dx.doi.org/10.3389/fneur.2020.546744>.
- [17] Meuschke M, Voß S, Gaidzik F, Preim B, Lawonn K. Skyscraper visualization of multiple time-dependent scalar fields on surfaces. *Comput Graph* 2021;99:22–42. <http://dx.doi.org/10.1016/j.cag.2021.05.005>.
- [18] Busking S, Botha CP, Ferrarini L, Milles J, Post FH. Image-based rendering of intersecting surfaces for dynamic comparative visualization. *Vis Comput* 2011;27(5):347–63. <http://dx.doi.org/10.1007/s00371-010-0541-z>.
- [19] Furmanová K, Jaresová M, Byska J, Jurčík A, Parulek J, Hauser H, Kozlíková B. Interactive exploration of ligand transportation through protein tunnels. *BMC Bioinform* 2017;18(S-2):1–16. <http://dx.doi.org/10.1186/s12859-016-1448-0>.
- [20] Hermann M, Schunke AC, Schultz T, Klein R. Accurate interactive visualization of large deformations and variability in biomedical image ensembles. *IEEE Trans Vis Comput Graph* 2016;22(1):708–17. <http://dx.doi.org/10.1109/tvcg.2015.2467198>.
- [21] Murugesan S, Bouchard K, Chang E, Dougherty M, Hamann B, Weber GH. Multi-scale visual analysis of time-varying electrocorticography data via clustering of brain regions. *BMC Bioinform* 2017;18(S6):1–15. <http://dx.doi.org/10.1186/s12859-017-1633-9>.
- [22] Glaßer S, Oeltze S, Preim U, Bjørnerud A, Hauser H, Preim B. Visual analysis of longitudinal brain tumor perfusion. In: Novak CL, Aylward S, editors. *SPIE proceedings*. SPIE; 2013, p. 86700Z. <http://dx.doi.org/10.1117/12.2007878>.
- [23] Smith MA, Nielsen CB, Chan FC, McPherson A, Roth A, Farahani H, Machev D, Steif A, Shah SP. E-scape: interactive visualization of single-cell phylogenetics and cancer evolution. *Nature Methods* 2017;14(6):549–50. <http://dx.doi.org/10.1038/nmeth.4303>.
- [24] Alves JM, Prieto T, Posada D. Multiregional tumor trees are not phylogenies. *Trends Cancer* 2017;3(8):546–50. <http://dx.doi.org/10.1016/j.trecan.2017.06.004>.
- [25] Reh A, Amirkhanov A, Kastner J, Gröller E, Heinzl C. Fuzzy feature tracking: Visual analysis of industrial 4D-XCT data. *Comput Graph* 2015;53:177–84. <http://dx.doi.org/10.1016/j.cag.2015.04.001>.
- [26] Diehl A, Pelorosso R, Ruiz J, Pajarola R, Gröller ME, Bruckner S. Hornero: Thunderstorms characterization using visual analytics. *Comput Graph Forum* 2021;40(3):299–310. <http://dx.doi.org/10.1111/cgf.14308>.
- [27] Alabi OS, Wu X, Harter JM, Phadke M, Pinto L, Petersen H, Bass S, Keifer M, Zhong S, Healey C, II RMT. Comparative visualization of ensembles using ensemble surface slicing. In: Wong PC, Kao DL, Hao MC, Chen C, Kosara R, Livingston MA, Park J, Roberts I, editors. *Visualization and data analysis 2012*. SPIE; 2012, p. 318–29. <http://dx.doi.org/10.1117/12.908288>.
- [28] Sugathan S, Bartsch H, Riemer F, Grüner ER, Lawonn K, Smit NN. Interactive multimodal imaging visualization for multiple sclerosis lesion analysis. In: *Eurographics workshop on visual computing for biology and medicine*. The Eurographics Association; 2021, p. 65–77. <http://dx.doi.org/10.2312/vcbm.20211346>.
- [29] Meier DS, Weiner HL, Guttmann CR. MR imaging intensity modeling of damage and repair in multiple sclerosis: Relationship of short-term lesion recovery to progression and disability. *Amer J Neuroradiol* 2007;28:1956–63. <http://dx.doi.org/10.3174/ajnr.A0701>.
- [30] Dale AM, Fischl B, Sereno MI. Cortical surface-based analysis. *NeuroImage* 1999;9(2):179–94. <http://dx.doi.org/10.1006/nimg.1998.0395>.
- [31] Woolrich MW, Jbabdi S, Patenaude B, Chappell M, Makni S, Behrens T, Beckmann C, Jenkinson M, Smith SM. Bayesian analysis of neuroimaging data in FSL. *Neuroimage* 2009;45(1):S173–86. <http://dx.doi.org/10.1016/j.neuroimage.2008.10.055>.
- [32] Reuter M, Rosas HD, Fischl B. Highly accurate inverse consistent registration: A robust approach. *NeuroImage* 2010;53(4):1181–96. <http://dx.doi.org/10.1016/j.neuroimage.2010.07.020>.
- [33] Reuter M, Schmansky NJ, Rosas HD, Fischl B. Within-subject template estimation for unbiased longitudinal image analysis. *NeuroImage* 2012;61(4):1402–18. <http://dx.doi.org/10.1016/j.neuroimage.2012.02.084>.
- [34] Klein S, Staring M, Murphy K, Viergever MA, Pluim J. Elastix: A toolbox for intensity-based medical image registration. *IEEE Trans Med Imaging* 2010;29(1):196–205. <http://dx.doi.org/10.1109/tmi.2009.2035616>.
- [35] Blender Online Community. Blender - a 3D modelling and rendering package. Stichting Blender Foundation, Amsterdam: Blender Foundation; 2018, URL: <http://www.blender.org>.
- [36] Saber M, Raz E. Dawson fingers. *Radiopaedia.org*; 2008. <http://dx.doi.org/10.53347/rid-1202>.
- [37] Harrower M, Brewer CA. ColorBrewer.org: An online tool for selecting colour schemes for maps. 2011, p. 261–8. <http://dx.doi.org/10.1002/9780470979587.ch34>.